X-ray diffuse scattering and conductivity studies of the N-methylphenazinium-tetracyanoquinodimethanide IA form

J. P. Pouget, S. Megtert, and R. Comès
Laboratoire de Physique des Solides, associé au Centre National de la Recherche Scientifique, Université Paris-Sud, Bâtiment 510, 91405 Orsay, France

A. J. Epstein
Xerox Webster Research Center, Rochester, New York 14644
(Received 29 March 1979)

The x-ray diffuse scattering study of the highly conducting form (IA) of N-methylphenazinium-tetracyanoquinodimethanide [(NMP)(TCNQ)] shows that the methyl groups, although less ordered than in the less highly conducting form (IB), still display substantial local order of the same type along the stacking a direction. In addition, it shows two types of one-dimensional (1-D) scattering bearing resemblance to the Kohn anomalies earlier observed in (TTF)(TCNQ). A first 1-D scattering is observed at room temperature at the wave vector $0.33a^*$; it couples three-dimensionally below approximately 200 K. Further diffuse scattering is observed below 70 K at half the previous wave vector ($0.165a^*$). As expected in an intrinsically disordered system (as potassium cyanoplatinate $[K_2Pt(CN)_4Br_{0.30}\cdot 3H_2O$ (KCP)]) no long-range 3-D ordering is observed down to 20 K. Our results cannot ascribe unambiguously the $0.33a^*$ and a $0.165a^*$ scattering to $4k_F$ and $2k_F$ anomalies (as was done for tetrathiafulvalenium-tetracyano-p-quinodimenthanide [(TTF)(TCNQ)]), but strongly suggests that the charge transfer in (NMP)(TCNQ) is 2/3 electron, and is quite far from unity as previously deduced from other work. Temperature-dependent dc conductivity measurements after x-ray study unequivalocally associate the highly conducting form with these properties.

I. INTRODUCTION

N-methylphenazinium-7,7,8,8-tetracyano-p-quinodimethanide [(NMP)(TCNQ)] was among the earliest known highly conducting organic quasi-one-dimensional (1-D) conductors.[1,2] Long before the more recently discovered examples of this family, it had been the center of considerable interest and controversy because of two features which still distinguish this compound from many of the others: (i) The asymmetric location of the methyl groups of the NMP molecules introduces an intrinsic static disorder,[3] (ii) the magnetic properties have been interpreted as resulting from very strong Coulomb interactions between electrons.[4] Various models have been proposed in an attempt to explain the temperature dependence of the electrical properties of (NMP)(TCNQ). These include (1) that (NMP)(TCNQ) is a semiconductor at all temperatures (T) studied, with an activated carrier concentration and a strongly temperature-dependent mobility,[5] (2) that the static disorder leads to localization of electronic wave functions to a small number of lattice sites, and conductivity occurs by hopping among these localized states,[6] and (3) assuming that there is a transfer of one electron from each NMP donor to each TCNQ acceptor, that this material has strong correlation between electrons and undergoes a Mott-Hubbard metal-insulator phase transition at the temperature of the maximum conductivity, $T_m = 230$ K.[4] The first model[5] emphasizes the applicability of a single transport model over a temperature range of 65 K $< T <$ 400 K with a second transport mechanism occurring below 65 K. The disorder[6] and metal-insulator transition[4] models emphasized that different transport mechanisms occurred above and below T_m. There has also been considerable interest and controversy concerning the exact fraction of charge transferred from NMP to TCNQ and its role in determining physical properties. Early workers assumed complete

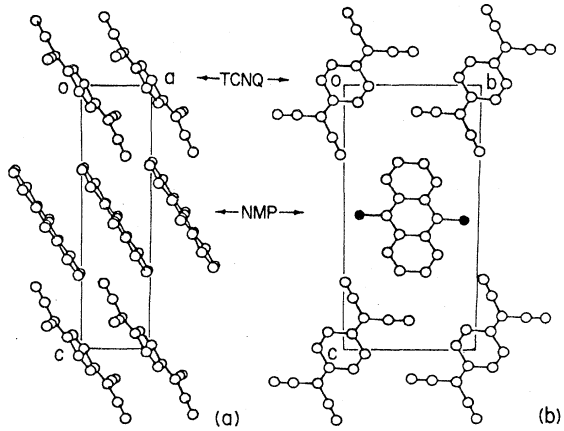

FIG. 1. Crystal structure of (NMP)(TCNQ)-I. (a) View down the b axis. (b) View down the highly conducting a axis. Note that two methyl groups are shown for each NMP molecule, indicating the randomness in the methyl group location. (From Fritchie, Ref. 3.)

charge transfer [$(NMP^+)(TCNQ^-)$],[4] while later contributors proposed incomplete charge transfer.[7-10]

(NMP)(TCNQ) was originally reported as crystallizing in two distinct stable forms: (i) a black highly conducting triclinic phase (NMP)(TCNQ)-I in which the donor and acceptor molecules form segregated stacks,[3] $a = 3.8682$ Å, $b = 7.7807$ Å, $c = 15.735$ Å, $\alpha = 91.67°$, $\beta = 92.71°$, $\gamma = 95.38°$, (see Fig. 1), and (ii) a purple semiconducting monoclinic phase (NMP)(TCNQ)-II which corresponds to $(NMPH^+)(TCNQ)^-$ in which donor [$(NMPH)^+$ or (N-methyl N-hydrophenazinium)$^+$] and acceptor molecules alternate in each stack[11,12] and which will not be considered here. The conducting form (NMP)(TCNQ)-I, according to recent investigations, can exist with two different degrees of disorder of the methyl groups. The most studied of these forms, which we shall call below (NMP)(TCNQ)-I*A*, shows an increasing conductivity as the temperature is lowered from 400 K to about 230 K, at which temperature the conductivity presents a broad maximum, then decreases rapidly as the temperature is decreased further,[4,5,13] displaying a behavior very similar to that of potassium cyanoplatinate [$K_2Pt(CN)_4Br_{0.3} \cdot 3.2H_2O$ (KCP) (Ref. 14)] under pressure.[15] On the basis of x-ray data the *IA* form was, until this study, assumed to correspond to a random disorder of methyl groups. Another less common and less well studied form, which we shall call below (NMP)(TCNQ)-I*B*, shows comparable values of room-temperature conductivity, but the conductivity decreases very rapidly with decreasing temperatures, and consequently does not pass through a maximum value below room temperature.[16] In this last form, diffuse x-ray scattering experiments showed that the methyl groups were ordered two dimensionally in the *ab* plans (*a* being the stacking direction), but without correlations between successive planes of this type.[17] In addition to the above, NMP and TCNQ also react to form $(NMP)(TCNQ)_2$ (Ref. 1) and $(NMP)_2(TCNQ)_3$.[18] The detailed chemical composition and structure of the different compounds of NMP with TCNQ has been the subject of considerable controversy.[19]

The present work concerns exclusively the highly conducting form (NMP)(TCNQ)-I*A*. The purpose of our study was twofold:

First, to try to characterize more precisely the order of the methyl groups, in comparison with the observation already reported on the less highly conducting (NMP)(TCNQ)-I*B*.

Second, to try to determine if the temperature dependence of conductivity can be associated with some kind of lattice distortion. Since the observation of a $4k_F$ scattering in (TTF)(TCNQ) (TTF is tetrathiafulvalenium) is generally (although there is considerable controversy) attributed to the existence of strong repulsive interactions between electrons, and (NMP)(TCNQ) is believed to be a compound with more pronounced electron correlations, the (NMP)(TCNQ) provides material for an additional test of the $4k_F$ scattering interpretation made for (TTF)(TCNQ).

Regarding the characterization of the disorder, we have found that the methyl groups of (NMP)-(TCNQ)-I*A* are not randomly disordered as earlier assumed, but ordered mainly along the *b* direction with only weak coupling in the (stacking) *a* direction, in contrast with (NMP)(TCNQ)-I*B*, where the methyl groups are ordered in both of these directions (*a*-*b* planes).[17]

Concerning the lattice distortion associated with the temperature dependence of the transport properties, we have observed in (NMP)(TCNQ)-I*A* two lattice distortions with wave vectors in the chain direction of $0.165a^*$ and $0.33a^*$, bearing some resemblance to the earlier observations in (TTF)(TCNQ).[20-22] We have also found that below around 200 K, the distortion waves begin to couple three dimensionally although no real long-range order is achieved down to 20 K. This behavior is similar to that of KCP which is another disordered 1-D conductor. Analysis of these distortion data leads to the conclusion that in (NMP)(TCNQ) a two-thirds charge is transferred from NMP to TCNQ.

II. EXPERIMENTAL

The experimental setup for the photographic study of x-ray diffuse scattering was similar to that previously used for the investigations of (TTF)(TCNQ).[20,22] Additional higher resolution photographs were taken at room temperature using the synchrotron radiation source of LURE at Orsay. Five (NMP)(TCNQ) single crystals, grown at the Xerox Webster Research Center with typical sizes of about $5 \times 0.02 \times 0.02$ mm^3 were used during this study. No difference in their diffuse x-ray pattern was observed. Temperature-dependent four-probe dc and low-frequency ac (13 Hz) conductivity measurements of one of these crystals established that they belong to form I*A*. The conductivity data, taken at the Webster Research Center, were taken at currents less than or equal to 10^{-6} A and care was taken to assure linear current-voltage relationships.

III. CHARACTERIZATION OF THE ORIENTATIONAL ORDER

The experimental observations are well summarized in the patterns of Figs. 2 and 3. These

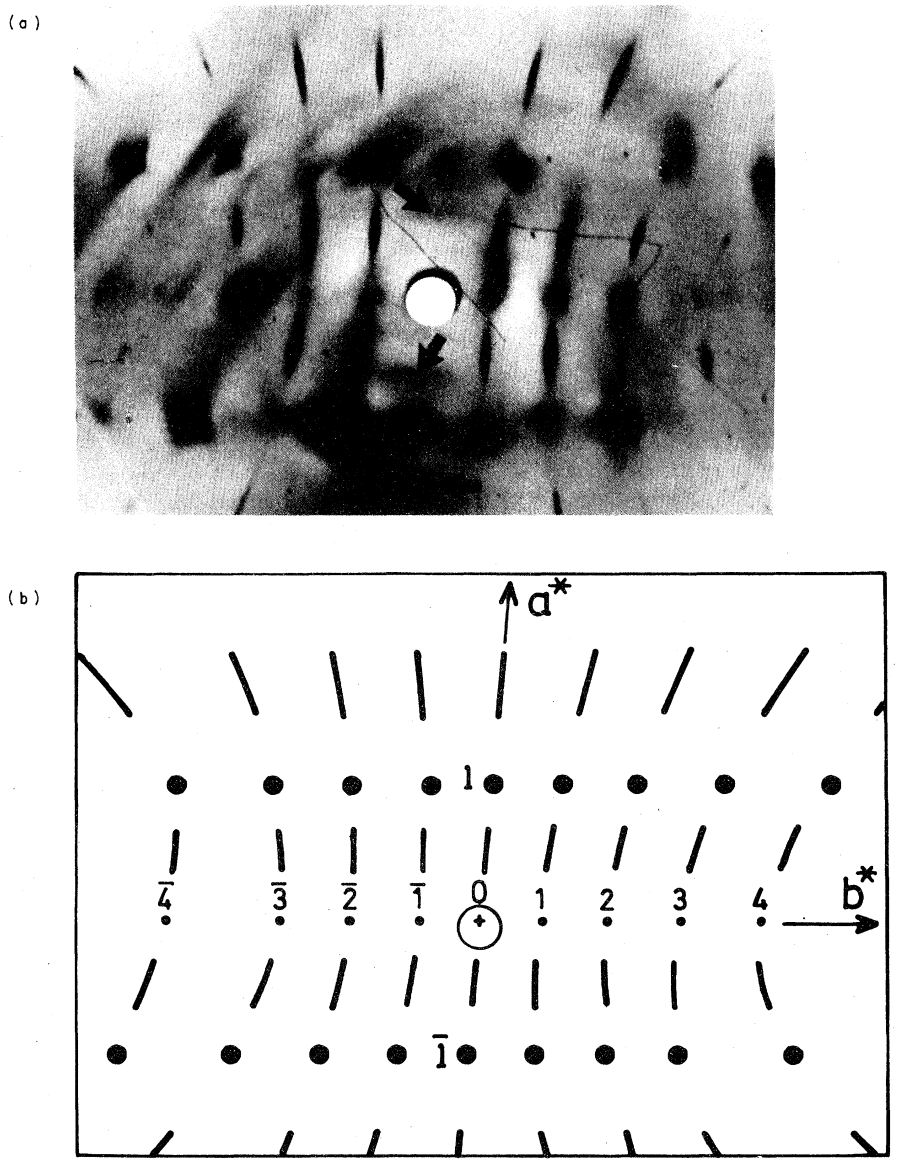

FIG. 2. (a) X-ray pattern of (NMP)(TCNQ)-I*A* at room temperature close to the (a^*, b^*) reciprocal plane, showing (i) the modulated (h, k_i, l) diffuse scattering related to the orientational disorder, as schematically indicated in part (b) of the Figure, and (ii) the 1-D scattering with wave-vector component $q_2 = \frac{1}{3}a^*$ (black arrow). The a^* and b^* directions are shown in part (b) and the x rays are approximately parallel to the c^* direction (streaking direction).

x-ray patterns are exceptionally complex since, superimposed on the usual diffraction from the main average lattice, there are two different types of diffuse scattering.

The strongest of these, which is temperature independent, is schematically shown in Fig. 2(b). It is located in reciprocal planes (h, k_i, l) perpendicular to the b direction (k_i is an integer). Within these planes, the intensity is only strongly dependent on h.

In this last direction the distribution of intensity presents *broad* maxima for $h = \frac{1}{2}(2n+1)$ (n integer) and can be well fitted by a Lorentzian line shape as shown in Fig. 4. This scattering is clearly related to the diffuse streaks in the c^* direction observed with (NMP)(TCNQ)-I*B*,[17] which, with the orientation presented in Fig. 2, would lead to *sharp* maxima for $h = \frac{1}{2}(2n+1)$. It can therefore be simply attributed to the orientational order of the NMP molecules. The difference observed be-

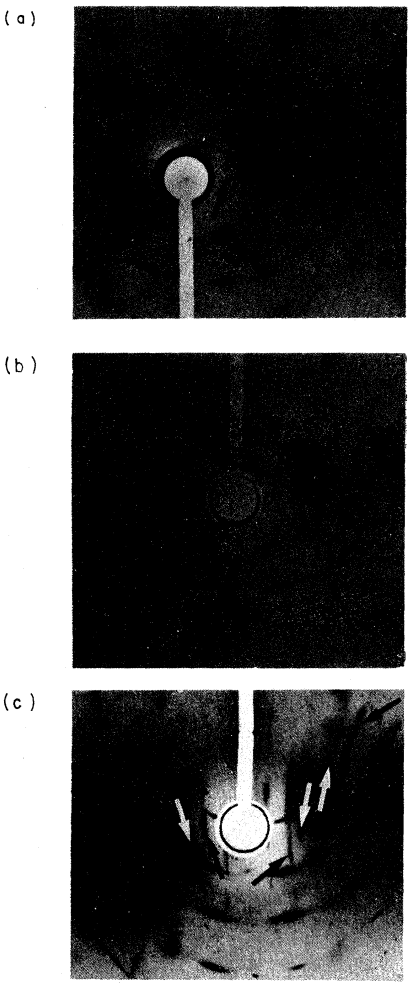

FIG. 3. (a) X-ray pattern of (NMP)(TCNQ) at 230 K showing the $q_2=\frac{1}{3}a^*$ satellite diffuse sheets. (b) X-ray pattern of (NMP)(TCNQ) at 120 K showing the building up of the 3-D order within the $q_2=\frac{1}{3}a^*$ satellite diffuse sheets. (c) X-ray pattern of (NMP)(TCNQ) at 20 K showing broad 3-D satellite reflections within the $q_2=\frac{1}{3}a^*$ and $q_1=\frac{1}{6}a^*$ satellite diffuse sheets. The black and white arrows point towards the $q_2=\frac{1}{3}a^*$ and $q_1=\frac{1}{6}a^*$ diffuse sheets, respectively. The x-rays have an arbitrary direction in the (b^*,c^*) plane; the a direction is horizontal.

tween highly conducting (NMP)(TCNQ)-I*A* of the present study and less highly conducting (NMP)(TCNQ)-I*B* is the much longer extension of the diffuse maxima in the a^* direction for (NMP)(TCNQ)-I*A*, contrasting with the sharp maxima in the b^* direction which seems to be common to both kinds of crystals. Using the observation of a diffuse intensity profile in the b^* direction, having, within experimental errors (~0.005 Å^{-1}) the experimental resolution, one obtains a lower limit of the correlation of the orientational order of the methyl groups in the b direction of ξ_b >200 Å (25 lattice constants). The (NMP)(TCNQ)-I*B* crystals show similar correlations of the methyl groups along the highly conducting a direction, forming, therefore, ordered a-b planes. In (NMP)(TCNQ)-I*A*, the alternation of the orientation of successive methyl groups on *chain direction* is only correlated over a few intermolecular spacings [the present study gives a value of ξ_a =25 Å (six lattice constants)] deduced from the Lorentzian scattering distribution shown in Fig. 4, after a Lorentzian correction due to the experimental resolution of 0.02 Å^{-1} (half width at half maximum: HWHM).

These observations lead to a first conclusion: The more highly conducting form of (NMP)(TCNQ)-I*A* is not randomly disorder as earlier assumed, but only less ordered than the less conducting form (NMP)(TCNQ)-I*B*. The correlation in the orientation of the NMP dipolar moments, based on dipole electrostatic forces considerations (alternation along the a axis and fixed orientation along the b direction) and deduced from the x-ray study of (NMP)(TCNQ)-I*B*,[17] remains valid for the (NMP)(TCNQ)-I*A* form. In both forms the NMP dipolar moments are found to be relatively well ordered in the b direction, the direction along which they are directed; they differ in the a direction along which the order is only local in (NMP)(TCNQ)-I*A*.

Striking is the fact that this more limited order in the higher conductivity form appears in the direction of high conductivity, the degree of order of the methyl groups seem therefore directly related to the different electrical properties. Re-

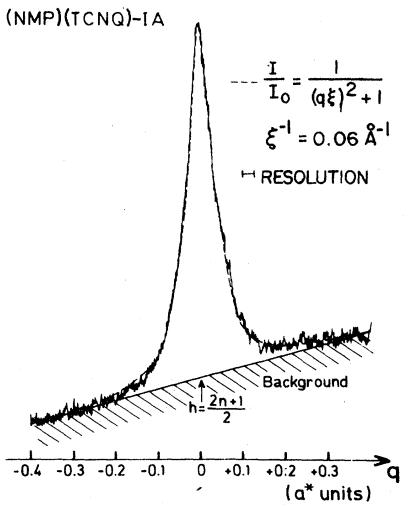

FIG. 4. Microdensitometer reading of a higher resolution photograph along the a^* direction, showing the h dependence of the diffuse streaks parallel to the c^* direction. The Lorentzian line shape fitting this distribution is also indicated.

ferring to semiconductor model for this system,[5] it is apparent that the system with greater disorder (I*A*) has a smaller energy gap. Assuming the same degree of charge transfer present in (NMP)(TCNQ)-I*A* and (NMP)(TCNQ)-I*B*, the decrease of the semiconducting energy gap with increasing disorder is consistent with previously noted behavior in three-dimensional[23,24] as well as one-dimensional[25] systems. From a metal-insulator transition viewpoint, the increased disorder observed here for (NMP)(TCNQ)-I*A* can, for example, inhibit the growth of charge-density waves in chain direction, and consequently push the conductivity maximum and the Peierls distortion toward a lower temperature compared to (NMP)(TCNQ)-I*B*.

IV. EVIDENCE FOR STRUCTURAL DISTORTIONS

A much weaker and temperature-dependent scattering is observed in planes perpendicular to the highly conducting a direction. This scattering, also visible in Fig. 2 at room temperature, is shown in Fig. 3 for three different lower temperatures, and has the aspect which has now become usual for the 1-D anomalies or lattice modulations found in other 1-D conductors.[20-22] Two different scatterings of this kind are observed respectively at the wave vector $q_1 = 0.165a^*$ and $q_2 = 0.33a^*$.

From room temperature to about 70 K, only the larger wave-vector scattering can be detected [Figs. 3(a) and 3(b)] showing that it cannot be considered as a second-order diffraction from the smaller wave-vector scattering. Below a temperature of about 70 K, the additional smaller-wave-vector scattering becomes visible [Fig. 3(c)]. Both types of scattering show increasing intensity with decreasing temperature in their respective temperature ranges.

The larger wave-vector scattering is already observable at room temperature, forming broad sheets at the $q_2 = (0.33 \pm 0.01)a^*$ position. These sheets sharpen progressively on cooling, as shown by the temperature dependence of the half width at half maximum (HWHM) represented in Fig. 5. With a Lorentzian resolution correction, the inverse HWHM yields for the q_2 scattering a correlation length ξ_{11} along the chain direction of 20 Å at 295 K and over 100 Å at 20 K. A similar resolution limited linewidth is also presented by the q_1 scattering at 20 K. It is interesting to remark that at low temperature, the q_1 and q_2 distortions spread over a distance in the chain direction, $\xi_{11} > 100$ Å, larger than that of the orientational disorder of the NMP molecules: $\xi_a \simeq 25$ Å. This indicates that the modulation in chain direction is not very sensitive to the NMP disorder and

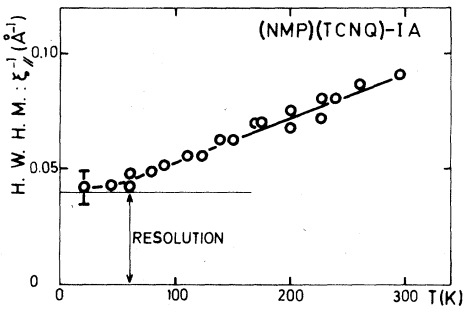

FIG. 5. Temperature dependence of the half width at half maximum (HWHM) for the $q_2 = 0.33a^*$ scatterings taken from the microdensitometer scans.

takes place on the TCNQ stacks and/or on the *averaged* NMP chains.

When the temperature is lowered, the q_2 scattering loses very progressively its 1-D character, and maxima of intensity within the $h = h_i \pm 0.33a^*$ satellite planes begin to be detected for temperatures around 200 K. These very broad maxima of intensity sharpen with decreasing temperature, but down to 20 K they never form well-defined satellite reflections. This behavior reflects a progressively increasing 3-D coupling between the q_2 waves on parallel chains in the two transverse directions, but which remains short range at 20 K. An estimate of the transverse correlation length at this temperature yields $\xi_\perp \simeq 30$ Å.

The q_1 scattering reveals similar broad maxima of intensity within the $h = h_i \pm 0.165a^*$ reciprocal layers. A noticeable difference is that the q_1 scattering never displays a truly 1-D character as weak 3-D coupling between the q_1 waves on parallel chains seems already present when this scattering becomes detectable below 70 K.

We have been unable to characterize precisely the type of 3-D coupling observed either for the q_1 or the q_2 scattering, the present fixed crystal fixed film technique being particularly inaccurate to determine the transverse components (in b and c directions) of the wave vector of satellite reflections in the particular case of (NMP)(TCNQ). This is because of the combined effects of the broadness of the diffuse spots and the poor resolution due to the focusing converging beam which does not allow a precise enough determination of the crystal orientation.

V. CONDUCTIVITY STUDIES

After having been temperature cycled several times from room temperature to 20 K in the x-ray study, the four-probe dc (or low-frequency, 13 Hz) conductivity measurement was performed on one of the samples. The sample was allowed

to cool very slowly (~1 K/3 min.) and data recorded at approximately 1 K intervals. A room-temperature conductivity of 100 $\Omega^{-1}\,cm^{-1}$ was measured. The normalized conductivity versus temperature graphs are shown in Figs. 6 and 7. The conductivity data for temperature less than 104 K have been multiplied by a factor of 1.67 to compensate for an irreversible decrease in conductivity σ, which occurred as the sample was cooled below this temperature. This probably was the result of irreversible fracturing of part of the crystal under the strains induced by thermal contraction. Figure 6 shows that the conductivity has a broad maximum around $T_m \sim 225$ K. The temperature-dependent derivative of the conductivity $-d\ln\sigma/dT^{-1}$ is shown in Fig. 8. (The derivative function was obtained by fitting the experimental data to a polynomial and analytically taking the derivative). The curve presents no sharp anomalies, but a smooth maximum around 40–80 K, followed above 80 K by a quasilinear behavior. This linear behavior for 80 K $< T <$ 300 K has been interpreted with a single charge transport mechanism without any change at T_m or elsewhere in this temperature range.[5,26] That is,[5] for 80 K $< T <$ 300 K,

$$-d\ln\sigma/dT^{-1} = \Delta_0 - \alpha T \,. \tag{1}$$

with Δ_0 and α constants. Integrating this expression, one obtains[5,26]

$$\sigma = \sigma_0 T^{-\alpha} \exp(-\Delta_0/T) \tag{2}$$

with σ_0 a constant. This parametrization has been interpreted[5,26] as representing the product of an activated carrier concentration present at all temperatures, and a strongly temperature-dependent mobility determined in large part by interaction with the molecular vibrations. The fit of Eq. (2) to the experimental conductivity data is best for Δ_0 850 K and for α 3.76. These results are consistent with values previously obtained[5] for (NMP)(TCNQ)-IA.

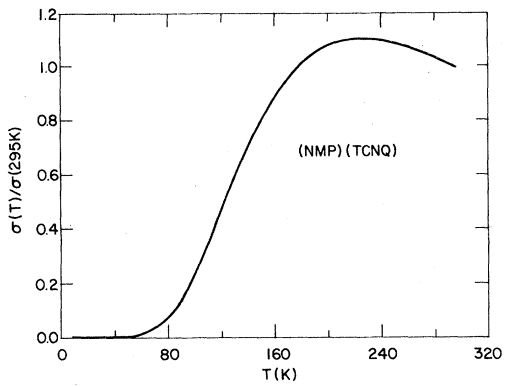

FIG. 6. Normalized four-probe a axis conductivity, $\sigma(T)/\sigma$ (295 K) versus temperature for one sample after cycling several times between room temperature and 20 K during x-ray studies. The $\sigma(T)$ data for $T < 104$ K were multiplied by 1.67 to compensate for an irreversible decrease in σ which occurred as the sample was cooled below this temperature.

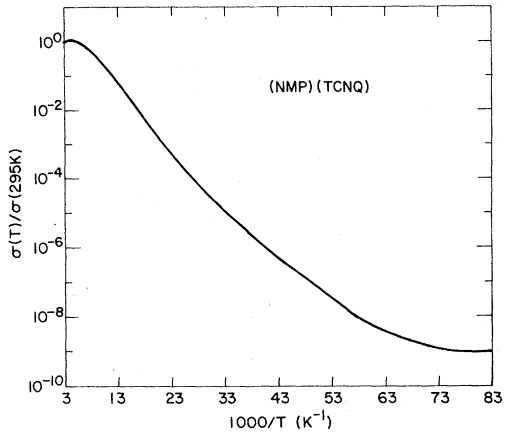

FIG. 7. Experimental $\log_{10}[\sigma(T)/\sigma(295\text{ K})]$ versus temperature for the sample studied in Fig. 6. The $\sigma(T)$ data for $T < 104$ K was multiplied by 1.67 to compensate for an irreversible decrease in σ which occurred as the sample was cooled below this temperature.

VI. DISCUSSION

We have already discussed briefly above the question of the characterization of the orientation order related to the transport properties. Below we shall therefore restrict the discussion to the structural aspects in relation to the lattice modulation of the Peierls type and its implication in understanding the degree of charge transferred from NMP to TCNQ and the electrical conductivity.

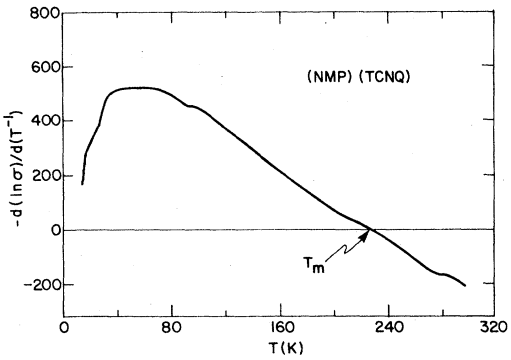

FIG. 8. Plot of $-d(\ln\sigma)/d(T^{-1})$ versus temperature for the (NMP)(TCNQ) data of Fig. 6. Above 80 K, note the continuous quasilinear behavior at temperatures above and below $T_m \sim 225$ K, the temperature of the maximum conductivity.

A. Interpretation of the structural data

The most important result of the present investigation is the observation of two kinds of scattering, i.e., of (static and/or dynamic) modulations in the chain direction. Although this recalls the case of (TTF)(TCNQ), one must be careful before a complete analogy can be made between the x-ray scattering results from the two compounds. In contrast with (TTF)(TCNQ), where the conduction band of the TTF and TCNQ stacks share a total of two electrons, in the case of (NMP)(TCNQ) there is only one electron available for charge transfer from each NMP molecule.

If we assume that both observed diffuse scatterings reflect the expected electron-phonon (or electron-lattice) coupling, this different situation allows several assignments for the anomalies observed respectively at the wave vectors $q_1=\frac{1}{6}a^*$ and $q_2=\frac{1}{3}a^*$.

Considering first the amount of charge transfer, there are already from the present structural data, two different possibilities: (A) $\frac{1}{3}$ electron per NMP molecule and $\frac{2}{3}$ electron per TCNQ molecules, and (B) $\frac{2}{3}$ electron per NMP molecule and $\frac{1}{3}$ per TCNQ molecule.

Taking further into account the type of electron bands from the two kinds of stacks, one gets the assignments summarized in Table I. If both kinds of stacks have normal electron bands for which two electrons of opposite spins can be accomodated per site (and which lead to the usual $2k_F$ Kohn anomalies), because of the single electron effectively available per NMP molecule, the Fermi wave vector is different for the NMP stacks and for the TCNQ stacks, and both kinds of scatterings can be assigned to $2k_F$ anomalies (Case I, Table I). If one deals with a Hubbard band (strong Coulomb interactions) on one type of chain leading to a $4k_F$ anomaly,[27] and a normal electron band of the other type of chain leading to a $2k_F$ anomaly, the two kinds of diffuse scattering can be attributed to $2k_F$ and $4k_F$ anomalies (Case II, Table I). Intermediate Coulomb interaction on one type of stack (leading to both $2k_F$ and $4k_F$ anomalies)[28] and a normal conduction band on the other stack (leading to a $2k_F$ anomaly alone) give rise to the assignments of Cases III and IV, Table I. Intermediate Coulomb repulsion on one type of stack and strong Coulomb correlations on the other type of chain leads to Case V. Case VI is for intermediate Coulomb repulsion on both types of stack, while Case VII is for intermediate Coulomb repulsion on one type of stack with $\frac{1}{3}$ electron per molecule, and no contribution from the other stack. Other cases which one can imagine, given the electron transfer of $\frac{1}{3}$ or $\frac{2}{3}$, are not com-

TABLE I. Allowed $2k_F$ and $4k_F$ assignments for (NMP)(TCNQ)-IA.

Case I: Normal band on both chains ($2k_F$ anomalies).

(A) TCNQ chain: $\rho=\frac{2}{3}$; $2k_F^{\mathrm{TCNQ}}=\frac{1}{3}a^*$

NMP chain: $\rho=\frac{1}{3}$; $2k_F^{\mathrm{NMP}}=\frac{1}{6}a^*$

(B) TCNQ chain: $\rho=\frac{1}{3}$; $2k_F^{\mathrm{TCNQ}}=\frac{1}{6}a^*$

NMP chain: $\rho=\frac{2}{3}$; $2k_F^{\mathrm{NMP}}=\frac{1}{3}a^*$

Case II: Strong Coulomb interaction on one chain ($4k_F$ anomaly). Normal band on the other chain ($2k_F$ anomaly).

(A) TCNQ chain: $\rho=\frac{2}{3}$; $4k_F^{\mathrm{TCNQ}}=\frac{2}{3}a^*$ ($\equiv\frac{1}{3}a^*$)

NMP chain: $\rho=\frac{1}{3}$; $2k_F^{\mathrm{NMP}}=\frac{1}{6}a^*$

(B) TCNQ chain: $\rho=\frac{1}{3}$; $2k_F^{\mathrm{TCNQ}}=\frac{1}{6}a^*$

NMP chain: $\rho=\frac{2}{3}$; $4k_F^{\mathrm{NMP}}=\frac{2}{3}a^*$ ($\equiv\frac{1}{3}a^*$)

Case III: Intermediate Coulomb interaction on one chain with $\frac{2}{3}$ electron in the conduction band ($2k_F$ and $4k_F$ anomalies). Normal band on the other chain ($2k_F$ anomaly).

(A) TCNQ chain: $\rho=\frac{2}{3}$; $4k_F^{\mathrm{TCNQ}}=\frac{2}{3}a^*$ and $2k_F^{\mathrm{TCNQ}}=\frac{1}{3}a^*$

NMP chain: $\rho=\frac{1}{3}$; $2k_F^{\mathrm{NMP}}=\frac{1}{6}a^*$

(B) TCNQ chain: $\rho=\frac{1}{3}$; $2k_F^{\mathrm{TCNQ}}=\frac{1}{6}a^*$

NMP chain: $\rho=\frac{2}{3}$; $4k_F^{\mathrm{NMP}}=\frac{2}{3}a^*$ and $2k_F^{\mathrm{NMP}}=\frac{1}{3}a^*$

Case IV: Intermediate Coulomb interaction on one chain with $\frac{1}{3}$ electron in the conduction band ($2k_F$ and $4k_F$ anomalies). Normal band on the other stack ($2k_F$ anomaly).

(A) TCNQ chain: $\rho=\frac{2}{3}$; $2k_F^{\mathrm{TCNQ}}=\frac{1}{3}a^*$

NMP chain: $\rho=\frac{1}{3}$; $4k_F^{\mathrm{NMP}}=\frac{1}{3}a^*$ and $2k_F^{\mathrm{NMP}}=\frac{1}{6}a^*$

(B) NMP chain: $\rho=\frac{1}{3}$; $4k_F^{\mathrm{NMP}}=\frac{1}{3}a^*$ and $2k_F^{\mathrm{NMP}}=\frac{1}{6}a^*$

TCNQ chain: $\rho=\frac{2}{3}$; $2k_F^{\mathrm{TCNQ}}=\frac{1}{3}a^*$

Case V: Intermediate Coulomb interaction on one chain with $\frac{1}{3}$ electron in the conduction band ($2k_F$ and $4k_F$ anomalies). Strong Coulomb interaction on the other chain.

(A) TCNQ chain: $\rho=\frac{2}{3}$; $4k_F^{\mathrm{TCNQ}}=\frac{2}{3}a^*$ ($\equiv\frac{1}{3}a^*$)

NMP chain: $\rho=\frac{1}{3}$; $4k_F^{\mathrm{NMP}}=\frac{1}{3}a^*$ and $2k_F^{\mathrm{NMP}}=\frac{1}{6}a^*$

(B) TCNQ chain: $\rho=\frac{1}{3}$; $4k_F^{\mathrm{TCNQ}}=\frac{1}{3}a^*$ and $2k_F^{\mathrm{NMP}}=\frac{1}{6}a^*$

NMP chain: $\rho=\frac{2}{3}$; $4k_F^{\mathrm{NMP}}=\frac{2}{3}a^*$ ($\equiv\frac{1}{3}a^*$)

Case VI: Intermediate Coulomb interaction on both chains ($2k_F$ and $4k_F$ anomalies).

(A) TCNQ chain: $\rho=\frac{2}{3}$; $4k_F^{\mathrm{TCNQ}}=\frac{2}{3}a^*$ and $2k_F^{\mathrm{TCNQ}}=\frac{1}{3}a^*$

NMP chain: $\rho=\frac{1}{3}$, $4k_F^{\mathrm{NMP}}=\frac{1}{3}a^*$ and $2k_F^{\mathrm{NMP}}=\frac{1}{6}a^*$

(B) TCNQ chain: $\rho=\frac{1}{3}$, $4k_F^{\mathrm{TCNQ}}=\frac{1}{3}a^*$ and $2k_F^{\mathrm{TCNQ}}=\frac{1}{6}a^*$

NMP chain: $\rho=\frac{2}{3}$, $4k_F^{\mathrm{NMP}}=\frac{2}{3}a^*$ and $2k_F^{\mathrm{NMP}}=\frac{1}{3}a^*$

TABLE I. *(Continued.)*

Case VII:	Intermediate Coulomb interaction on one chain with $\frac{1}{3}$ electron in the conduction band ($2k_F$ and $4k_F$ anomalies). No contribution from the other chain.
(A) TCNQ chain:	$\rho=\frac{2}{3}$; no diffuse scattering.
NMP chain:	$\rho=\frac{1}{3}$; $4k_F^{NMP}=\frac{1}{3}a^*$ and $2k_F^{NMP}=\frac{1}{6}a^*$
(B) TCNQ chain:	$\rho=\frac{1}{3}$; $4k_F^{TCNQ}=\frac{1}{3}a^*$ and $2k_F^{TCNQ}=\frac{1}{6}a^*$
NMP chain:	$\rho=\frac{2}{3}$; no diffuse scattering.

patible with the experimental observations.

The case of a chain with $\frac{2}{3}$ of an electron in the conduction band provides a very special situation which may be of theoretical interest. For the stacks which correspond to the conduction band with $\frac{2}{3}$ electron per molecule, $4k_F$ and $2k_F$ anomalies occur in the reduced zone at the same wave vector; in other words, $2k_F$ and $4k_F$ processes cannot be distinguished. Thus there is no real difference between the cases I, II, III and between the cases IV, V, VI, leading only to three distinct classes of solution:

class 1: case I or II or III,
class 2: case IV or V or VI,
class 3: case VII.

Because of all these compatible assignments and the very special values of the electron transfer, our study cannot state unambiguously the presence of strong Coulomb interactions between electrons in (NMP)(TCNQ).

B. Comparison with other physical properties

Regardless of which of the above possible assignments really applies to highly conducting (NMP)(TCNQ), with the interpretation of the present x-ray diffuse scattering results in terms of electron-phonon coupling, we end up with $\frac{1}{3}$ or possibly $\frac{2}{3}$ electron per molecule remaining on the NMP stacks. These values are very different from the charge transfer which was most often inferred from other and more indirect measurements, that is to say, nearly 1 electron per molecule on the TCNQ stacks (i.e., almost no noncore electron left in the NMP stacks). Among others[7-10] one has in particular to mention nuclear-magnetic-resonance experiments,[9] but there the deduced value of the charge transfer depends strongly upon the calculated spin-density distribution and can therefore not be considered as absolutely accurate; the best compatibility between these calculations from the NMR measurements and the present structural data is a charge transfer of $\frac{2}{3}$ electron (i.e., $\frac{1}{3}$ electron per molecule left on the NMP stacks). Indeed, we note that the thermoelectric power S for (NMP)(TCNQ) (Ref. 10) is nearly identical with that of $(N(CH_3)_3H)(I)$(TCNQ),[29,30] which is known[29] to have $\frac{2}{3}$ electron per TCNQ. Conductivity,[31] thermoelectric power,[32] and magnetic susceptibility[33] studies of variable charge transfer in the (NMP)(TCNQ) structure using the $(NMP)_x$ (phenazine)$_{1-x}$(TCNQ) system,[34] $0.5 \leq x \leq 1.0$, demonstrate that (NMP)(TCNQ) has significantly greater than 0.5 charge per TCNQ.

Much smaller values for the charge transfer have, however, been considered in other studies. An examination of measured bond lengths in a variety of 1-D conductors led to an estimated charge transfer of about 0.42 electrons,[35] and a theoretical model explicitly worked out for (NMP)(TCNQ), and based on strong Coulomb interactions between electrons predicts a charge transfer of 0.2 to 0.5 electron.[36] As these results are relatively inaccurate and more model dependent than those referred to in the previous paragraph, it appears reasonable to conclude that there are $\frac{2}{3}$ electron per TCNQ in (NMP)(TCNQ)-I*A*. In this case, the $q_1=\frac{1}{6}a^*$ scattering *must* be attributed to the NMP stack and any $2k_F$ or $4k_F$ modulation of the TCNQ stack will affect only the $q_2=\frac{1}{3}a^*$ scattering. This corresponds to all cases A in Table I.

It is, of course, possible to imagine another origin (not related to the expected electron-phonon coupling in such 1-D conductors) for the observed x-ray diffuse scattering, but this appears unlikely because the structural results are so similar to the effect of charge-density waves in other 1-D conductors.

The impact of these diffuse x-ray and conductivity results on understanding the applicability of various models for charge transport is substantial. As stated in the Introduction, three distinct models have been proposed for (NMP)(TCNQ). First, the lack of complete charge transfer establishes that (NMP)(TCNQ) cannot undergo a simple Mott-Hubbard phase transition, which only occurs for exactly one charge per site.

Second, the observation of a 1-D scattering at $q_2=\frac{1}{3}a^*$ is direct evidence for the existence, on the TCNQ stack at least, of a well-defined Fermi wave vector. This could only come about through delocalized electronic wave functions, in contradiction to the thesis of disordered based models. In addition, as noted above, the $q_1=\frac{1}{6}a^*$ is almost certainly associated with the NMP stack. This demonstrates a well-defined Fermi wave vector even on a stack with disorder. That is, the electronic wave functions must be considerably delocalized even on the chain in which the disorder effect would be expected to be the strongest.

Hence, these disorder models should be used only in establishing the effects of a small number of localized states as in a mobility edge. The experimental results given above show that the continuous building up of 3-D coupling of the $\frac{1}{3}a^*$ wave-vector modulation around 200 K appears in the same temperature range where the electrical conductivity is decreasing (the conductivity maximum occurs at 225 K, Fig. 6). For comparison, a correlation between the onset of 3-D ordering and the drop of electrical conductivity was also noticed in (TTF)(TCNQ).[22] The development around 70 K of an additional 3-D coupled q_1 wave-vector modulation further corresponds to a well established change in the temperature dependence of the electrical conductivity of (NMP)(TCNQ)-*IA*,[5] as shown in Fig. 8. Thus, the change in the temperature variations of $\sigma(T)$ at 70 K might be associated with the onset of this new 3-D ordering and reveal the appearance of a new "phase," whose transition temperature is not well defined because of the disorder and which might correspond, for example, to a Peierls state in which both stacks are distorted. However, because of the smoothness of the temperature variations of $\sigma(T)$, one cannot exclude a change in transport mechanism coincidentally occurring at this temperature. For example, activation of charge carriers to the conduction band from localized states in the gap may, around 70 K, begin to dominate excitations of carriers from the valence band to the conduction band.[31]

These diffuse scattering results are also consistent with the semiconductor model previous developed for (NMP)(TCNQ).[5] In this model a single transport mechanism is involved for the temperature region of 70 K $< T <$ 400 K, with the presence of an activated carrier concentration. Fits to the conductivity data[5] have been done with a single activation energy Δ_0 for this temperature range. It has been pointed out earlier[5] that it is not possible to distinguish between a constant activation energy Δ_0 and one that varies slowly with temperature. That is, if a temperature-dependent activation energy Δ were given by $\Delta = \Delta_0 - \beta T - \gamma T \ln T$, the conductivity parametrization given by Eq. (2) would still be effective, but the interpretation of the constants obtained may change. The structural evidences of charge-density waves in (NMP)(TCNQ) strongly suggest that the activation energy Δ might be related to a Peierls-type energy gap or to a relatively well-pronounced pseudogap. The observation of a relatively long correlation length in the 1-D regime[37] ($\xi_{11} \sim 5a$ at room temperature) which increases smoothly when the temperature decreases (Fig. 5), the development of a 3-D chain coupling[38] around 200 K, together with the possible formation of mobility edge by the NMP disorder are in favor of the presence of a relatively well-defined energy gap or pseudogap on the TCNQ chains.

A remarkable feature is that, at low temperature, the 3-D coupling between q_1 and q_2 waves does not achieve long-range order; this clearly confirms the secondary role of disorder previously assumed for the similar behavior observed with KCP, i.e., the phase of the waves (whether $4k_F$ or $2k_F$) are pinned by the disorder which prevents long-range ordering.[39]

Another type of diffuse scattering at $(h_i \pm 0.094n)a^*$ (n integer, varying from 0 to 5) was recently reported and attributed to k_F, $2k_F$, $4k_F$, $6k_f$, . . . scatterings in less highly conducting (NMP)(TCNQ)-*IB*.[40] The observation of so many orders (and perhaps most particularly $0k_F$) seems incompatible with an explanation in terms of Kohn anomalies, at least as measured so far. In highly conducting (NMP)(TCNQ)-*IA* of the present study, we could not observe such a type of scattering in any of the studied samples.[41]

ACKNOWLEDGMENTS

The authors are indebted to D. J. Sandman and J. S. Miller for providing samples for this study. The authors of this work have benefited from many valuable discussions, especially those with J. Bardeen, J. Bray, P. M. Chaikin, E. Conwell, V. Emery, A. F. Garito, A. J. Heeger, D. Jérome, P. Pincus, and M. J. Rice.

[1] L. R. Melby, Can. J. Chem. 43, 1448 (1965).
[2] I. F. Shchegolev, Phys. Status Solidi B 12, 4 (1972).
[3] C. J. Fritchie, Acta Crystallogr. 20, 892 (1966); B. Morosin, Phys. Lett. 53A, 455 (1975).
[4] A. J. Epstein, S. Etemad, A. F. Garito, and A. J. Heeger, Solid State Commun. 9, 1803 (1971); Phys. Rev. B 5, 952 (1972).
[5] A. J. Epstein, E. M. Conwell, D. J. Sandman, and J. S. Miller, Solid State Commun. 23, 355 (1977).
[6] A. M. Bloch, R. B. Weisman, and C. M. Varma, Phys. Rev. Lett. 28, 753 (1972).
[7] Z. G. Soos, Annu. Rev. Phys. Chem. 25, 121 (1974).
[8] J. B. Torrance, B. A. Scott, and F. B. Kaufman, Solid State Commun. 17, 1369 (1975).
[9] M. A. Butler, F. Wudl, and Z. G. Soos, Phys. Rev. B 12, 4708 (1975); F. Devreux, M. Guglielmi, and

M. Nechtschein, J. Phys. (Paris) 39, 541 (1978).
[10]J. F. Kwak, G. Beni, and P. M. Chiakin, Phys. Rev. B 13, 641 (1976).
[11]B. Morosin, Acta. Crystallogr. Sec. B 32, 1176 (1976); 34, 1905 (1978).
[12]Z. G. Soos, H. J. Keller, W. Moroni, and D. Nöthe, J. Am. Chem. Soc. 99, 5040 (1977).
[13]L. B. Coleman, J. A. Cohen, A. F. Garito, and A. J. Heeger, Phys. Rev. B 7, 2122 (1973).
[14]J. S. Miller and A. J. Epstein, Prog. Inorg. Chem. 20, 1 (1976).
[15]M. Thielmans, R. Deltour, D. Jérome, and J. R. Cooper, Solid State Commun. 19, 21 (1976).
[16]G. Fujii, I. Shirotani, and H. Nagano, Bull. Chem. Soc. Jpn. 50, 1726 (1977).
[17]H. Kobayashi, Bull. Chem. Soc. Jpn. 48, 1373 (1975).
[18]F. Sanz and J. J. Daly, J. Chem. Soc. Perkin Trans. 2, 1146 (1975).
[19]D. J. Sandman, J. Am. Chem. Soc. 100, 5230 (1978).
[20]J. P. Pouget, S. K. Khanna, F. Denoyer, R. Comès, A. F. Garito, and A. J. Heeger, Phys. Rev. Lett. 37, 437 (1976).
[21]S. Kagoshima, T. Ishiguru, and H. Anzai, J. Phys. Soc. Jpn. 41, 2061 (1976).
[22]S. K. Khanna, J. P. Pouget, R. Comes, A. F. Garito, and A. J. Heeger, Phys. Rev. B 16, 1468 (1977).
[23]J. E. Fischer, M. Glicksman, and J. A. Van Vechten, in *Proceedings of the 13th International Conference on the Physics of Semiconductors*, Rome, Italy, 1976, edited by F. G. Fumi (North-Holland, Amsterdam, 1976).
[24]J. A. Van Vechten and T. K. Bergstresser, Phys. Rev. B 1, 3351 (1970).
[25]G. Mihály, G. Said, G. Grüner, and M. Kertész, Solid State Commun. 21, 1115 (1977).
[26]A. J. Epstein, E. M. Conwell, and J. S. Miller, Ann. N. Y. Acad. Sci. 313, 183 (1978); A. J. Epstein and E. M. Conwell, Solid State Commun. 24, 627 (1977).
[27]J. Bernasconi, M. J. Rice, W. R. Schneider, and S. Strassler, Phys. Rev. B 12, 1090 (1975); V. J. Emery, Phys. Rev. Lett. 37, 107 (1976); J. B. Torrance, Phys. Rev. B 17, 3099 (1978); J. R. Fletcher and G. A. Toombs, Solid State Commun. 22, 2984 (1977); P. A. Lee, T. M. Rice, and R. A. Klemm, Phys. Rev. B 15, 2984 (1977); J. Kondo and K. Yamaji, J. Phys. Soc. Jpn. 43, 424 (1977); J. Hubbard, Phys. Rev. B 17, 494 (1978).
[28]See, for example, V. J. Emery, in *Chemistry and Physics of One-Dimensional Metal*, edited by H. J. Keller (Plenum, New York, 1977).
[29]M. Abkowitz, J. W. Brill, P. M. Chaikin, A. J. Epstein, M. F. Froix, C. H. Griffiths, W. Gunning, A. J. Heeger, W. A. Little, J. S. Miller, M. Novatny, D. B. Tanner, and M. L. Slade, Ann. N. Y. Acad. Sci. 313, 459 (1978).
[30]P. M. Chaikin, A. J. Epstein, and J. S. Miller (unpublished).
[31]A. J. Epstein and J. S. Miller, Solid State Commun. 27, 325 (1978).
[32]A. J. Epstein, J. S. Miller, and P. M. Chaikin, Phys. Rev. Lett. 43, 1178 (1979).
[33]A. J. Epstein and J. S. Miller (unpublished).
[34]J. S. Miller and A. J. Epstein, J. Am. Chem. Soc. 100, 1639 (1978).
[35]S. Flandrois and D. Chasseau, Acta. Crystallogr. Sec. B 33, 2744 (1977).
[36]A. A. Ovchinnikov, M. Ya. Krivnov, V. E. Klymenko, and I. I. Ukrainsky in *Organic Conductors and Semiconductors*, Lecture Notes in Physics (Springer, New York, 1977), Vol. 65, p. 103.
[37]P. A. Lee, T. M. Rice, and P. W. Anderson, Phys. Rev. Lett. 31, 462 (1973).
[38]M. J. Rice and S. Strassler, Solid State Commun. 13, 1389 (1973).
[39]P. A. Lee, T. M. Rice, and P. W. Anderson, Solid State Commun. 15, 703 (1974).
[40]K. Ukei and I. Shirorani, Comments on Solid State Phys. 2, 159 (1977).
[41]Preliminary measurements performed on a different batch of (NMP)(TCNQ) samples, grown at Nancy by P. Dupuis, which possess some of the characters of the (NMP)(TCNQ)-IB form, reveal in addition to the q_1 and q_2 scattering described in this paper, scatterings at $q \sim n \times 0.1\, a^*$ $(n = 1, 2, \ldots)$ which might bear some resemblance with that reported in Ref. 40. However, this scattering, decreasing with lowering temperature, behaves as "usual" thermal scattering which makes it a very unlikely candidate for a phonon anomaly, which is expected to sharpen towards lower temperatures. [J. P. Pouget, S. Megtert, and R. Comès, in *Proceedings of the International Conference on Quasi* 1-D *Conductors, Dubrovnik, 1978*, Springer Lecture Notes in Physics, edited by S. Barišić, *et al.* (Springer, Berlin, 1979), Vol. 95, p. 14].

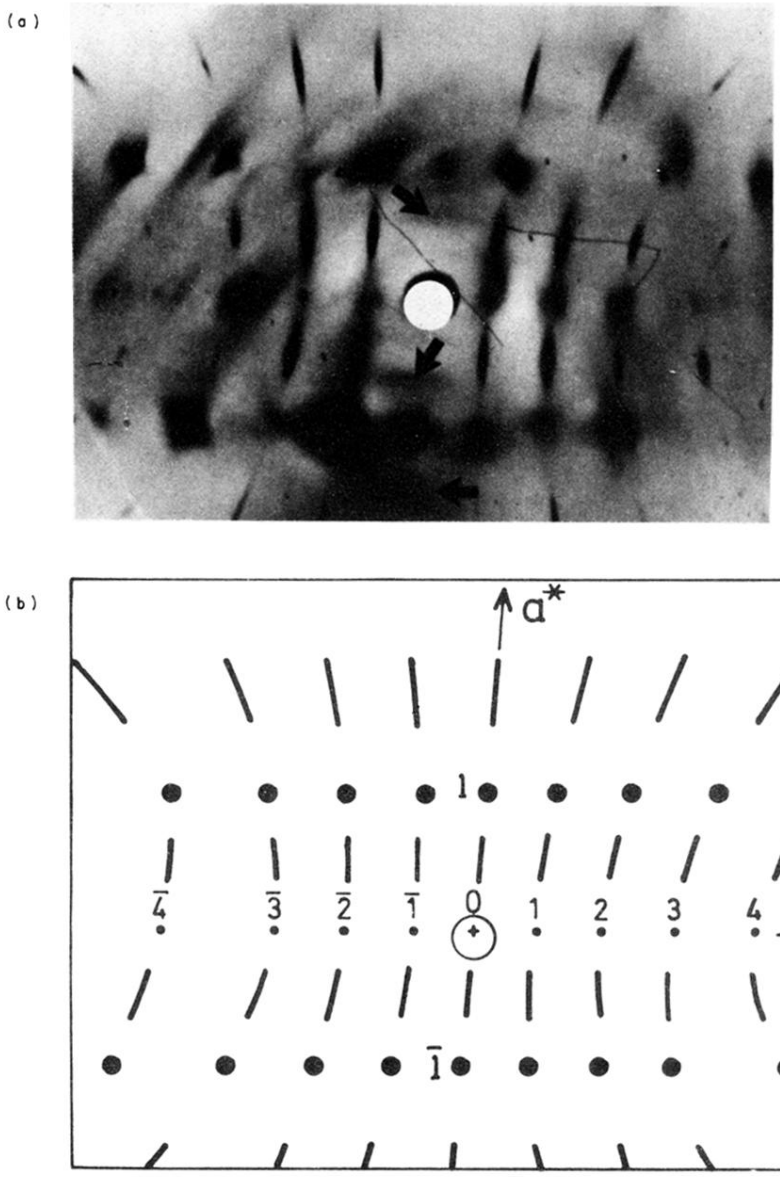

FIG. 2. (a) X-ray pattern of (NMP)(TCNQ)-*IA* at room temperature close to the (a^*, b^*) reciprocal plane, showing (i) the modulated (h, k_i, l) diffuse scattering related to the orientational disorder, as schematically indicated in part (b) of the Figure, and (ii) the 1-D scattering with wave-vector component $q_2 = \frac{1}{3}a^*$ (black arrow). The a^* and b^* directions are shown in part (b) and the x rays are approximately parallel to the c^* direction (streaking direction).

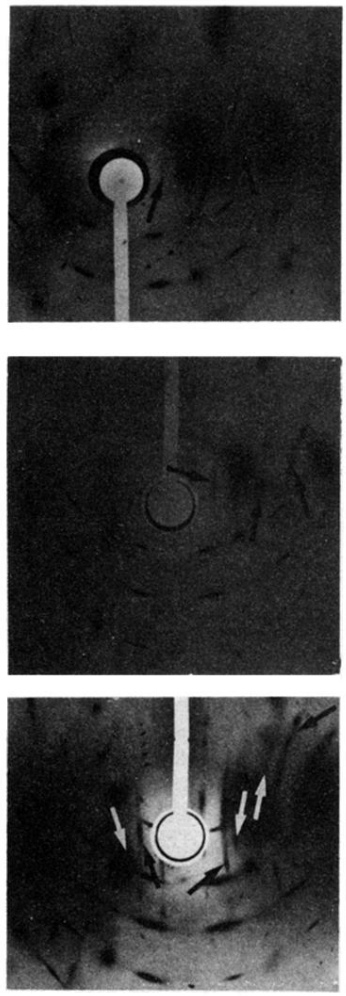

FIG. 3. (a) X-ray pattern of (NMP)(TCNQ) at 230 K showing the $q_2=\frac{1}{3}a^*$ satellite diffuse sheets. (b) X-ray pattern of (NMP)(TCNQ) at 120 K showing the building up of the 3-D order within the $q_2=\frac{1}{3}a^*$ satellite diffuse sheets. (c) X-ray pattern of (NMP)(TCNQ) at 20 K showing broad 3-D satellite reflections within the $q_2=\frac{1}{3}a^*$ and $q_1=\frac{1}{6}a^*$ satellite diffuse sheets. The black and white arrows point towards the $q_2=\frac{1}{3}a^*$ and $q_1=\frac{1}{6}a^*$ diffuse sheets, respectively. The x-rays have an arbitrary direction in the (b^*, c^*) plane; the a direction is horizontal.